

Radio Cherenkov signals from the Moon: neutrinos and cosmic rays

Yu Seon Jeong and Mary Hall Reno

Department of Physics and Astronomy, University of Iowa, Iowa City, IA 52242

Ina Sarcevic

Department of Physics, University of Arizona, Tucson, AZ 85721

Department of Astronomy and Steward Observatory, University of Arizona, Tucson, AZ 85721

Neutrino production of radio Cherenkov signals in the Moon is the object of radio telescope observations. Depending on the energy range and detection parameters, the dominant contribution to the neutrino signal may come from interactions of the neutrino on the Moon facing the telescope, rather than neutrinos that have traversed a portion of the Moon. Using the approximate analytic expression of the effective lunar aperture from a recent paper by Gayley, Mutel and Jaeger, we evaluate the background from cosmic ray interactions in the lunar regolith. We also consider the modifications to the effective lunar aperture from generic non-standard model neutrino interactions. A background to neutrino signals are radio Cherenkov signals from cosmic ray interactions. For cosmogenic neutrino fluxes, neutrino signals will be difficult to observe because of low neutrino flux at the high energy end and large cosmic ray background in the lower energy range considered here. We show that lunar radio detection of neutrino interactions is best suited to constrain or measure neutrinos from astrophysical sources and probe non-standard neutrino-nucleon interactions such as microscopic black hole production.

I. INTRODUCTION

Ultrahigh energy neutrinos may originate from astrophysical sources, from exotic sources such as ultramassive particles which decay and from cosmic ray interactions with the background radiation [1]. Because cosmic rays have been observed up to energies of 10^{19} eV, high energy neutrino flux from cosmic ray interactions with photons producing charged pions [2] which decay into neutrinos [3] is a “guaranteed” neutrino flux. Detailed flux predictions of these final state neutrinos, called GZK-neutrinos or cosmogenic neutrinos, still have theoretical uncertainties associated with the composition and injection spectrum of the highest energy cosmic rays, and the photon spectrum now and at earlier epochs, as discussed in, e.g., Refs. [4–9]. Observations of neutrino signals will be an important piece of the high energy astrophysics and cosmological picture.

In contrast to photons, neutrinos have weak interaction cross sections [10–14] so neutrino fluxes are not attenuated over cosmic distances. However, one needs detectors sensitive to many targets for neutrino interactions since the interaction probability is low. There are already a number of efforts to observe these highest energy neutrinos, including signals from the air showers they would produce [15], and from the particles and radiation they produce when they interact in matter [16–25]. All observational efforts require large volumes.

Among these observational efforts are neutrino induced events on the Moon, where the Moon is the target, and the signal is the radio Cherenkov emission [19–25]. Neutrinos, when they interact with nucleons and nuclei, generate hadronic showers with shower energies of $E_{\text{shr}} \simeq 0.2E_\nu$. An electron charge excess is produced,

and this group of electrons moves faster than the speed of light in the lunar regolith, hence the Cherenkov signal [26].

Evaluation of the signal depends on the cosmogenic neutrino flux, the ultrahigh energy neutrino cross section, the radio signal production, attenuation and refraction at the surface and detection parameters. An approximate expression for the effective aperture for neutrino induced radio Cherenkov signals from the Moon has been developed by Gayley, Mutel and Jaeger (GMJ) in Ref. [27]. Ultrahigh energy neutrinos are incident isotropically on the Moon to a good approximation. In analogy with terrestrial observations, e.g., at the IceCube neutrino observatory [28], neutrinos that are incident on the “back-side” of the Moon and traverse a portion of the Moon before interacting are called “upward” neutrinos. Neutrinos which interact on the surface of the Moon facing the Earth are denoted “downward” neutrinos.

Gayley et al. find that, depending on the energy and cross section, the event rate from neutrinos incident on the surface we see (downward neutrinos) sometimes dominates over the event rate from neutrinos incident on the surface of the Moon not visible from Earth (upward neutrinos) [27]. This may seem counter-intuitive, however, between the various angles of incidence, the Cherenkov angle and the angular spread of the Cherenkov cone, angles of refraction and angle characterizing the lunar surface roughness, the downward neutrinos can contribute appreciably to the signal.

Cosmic ray interactions in the lunar regolith produce hadronic showers as well. These cosmic ray induced hadronic showers also induce a charge excess and a related radio Cherenkov signal which can be used to measure or constrain the ultrahigh energy cosmic ray flux

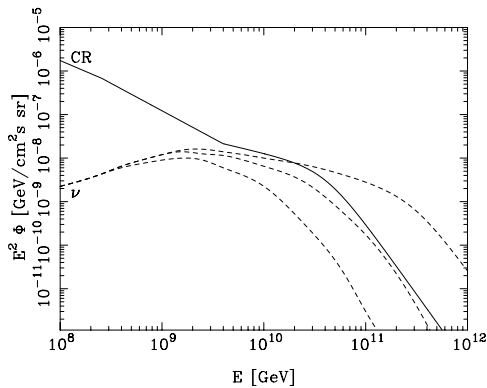


FIG. 1: The flux of cosmic rays (solid) with the parametrization from Ref. [30] and three models for the flux of cosmogenic neutrinos (dashed) from Ref. [9] with the assumption of proton primaries.

[29]. The cosmic ray flux is quite large at low energy, but it falls off rapidly with increasing energy. The flux of cosmic rays (solid line) and three models for the flux of cosmogenic neutrinos from Ref. [9] (dashed lines) are shown in Fig. 1. The three models for the cosmogenic neutrinos are a subset of predictions for the cosmogenic neutrino flux. These three come from the initial assumption of cosmic rays which are primarily protons, in which the sources are assumed to have maximum acceleration energies of $E_{p,max} = 10^{11}$ GeV, $10^{11.5}$ GeV and 10^{12} GeV. Details of the model, including injection spectra, assumptions about the star formation rate and the correlated UHE cosmic ray sources and other inputs to the evaluation are described in Ref. [9]. The cosmic ray flux shown uses the parametrization of the Auger Collaboration in Ref. [30].

Given the cosmic ray flux [30] and its production of radio Cherenkov signals similar to the corresponding neutrino Cherenkov signals [29], we evaluate the cosmic ray induced signals. The considerations for cosmic rays, as compared to neutrinos, are somewhat different. Cosmic ray fluxes are attenuated in the Earth’s atmosphere, however, there is no lunar atmosphere. Within the lunar regolith, the cosmic ray interaction length is small compared to any other characteristic distance scale. There will not be any “upward” cosmic ray induced signals, but there is the potential for “downward” cosmic rays to produce radio Cherenkov signals. Cosmic ray flux attenuation in the lunar regolith is, of course, a large effect, resulting in cosmic ray signals being produced very close to the lunar surface. In Ref. [29], ter Veen *et al.* have determined that the radio Cherenkov signal far from the lunar surface is essentially the same as one originating deeper in the regolith (apart from attenuation).

In this paper, we look at the relative importance of

cosmic ray and neutrino induced radio Cherenkov signals from the Moon assuming standard model cross sections and the neutrino and cosmic ray fluxes in Fig. 1. We use the approximate expression from Ref. [27] for the event rates, and we modify this analytic result to account for strong attenuation where applicable. We also consider non-standard model neutrino-nucleon cross sections and generic neutrino fluxes from astrophysical sources.

There have been a number of discussions of the cross section dependence of various neutrino induced signals [31–33]. In the next section, we review the neutrino cross section and the resulting dependence of the event rate on the cross section. In Section III, we evaluate the event rates using the standard model neutrino nucleon cross section and for some rescaled cross sections, all using the approximate analytic GMJ expression of Ref. [27]. The dependence of the event rate on detection characteristics, namely the radio frequency and minimum detectable electric field, is shown.

In Section IV, we show how the approximate analytic expression is modified to account for cosmic ray flux attenuation on short distance scales in the lunar regolith. We find that the event rate is independent of cosmic ray cross section, as long as the cosmic ray interaction length is small compared to the photon attenuation length. We compare the rates of cosmic ray and neutrino induced radio signals using the fluxes shown in Fig. 1 and the standard model neutrino nucleon cross section. We show in Section V how the inclusion of mini-black hole production, as an example of a neutrino-nucleon cross section enhancement, and how alternative neutrino spectra affect the predicted event rates.

Our conclusions appear in Section VI. We find that while lowering the minimum electric field detectable by a radio telescope array would help increase the number of neutrino events, since it effectively lowers the neutrino energy threshold for detection, it also increases the number of cosmic ray events. Cosmogenic neutrino fluxes on the scale of those presented in Ref. [9] will be difficult to observe on the one hand because of low fluxes (at the high energy end) or because of the cosmic ray background (in the lower energy range considered here). Lunar radio detection of neutrino interactions is best suited to constrain or measure neutrino sources other than the cosmogenic sources and non-standard neutrino nucleon cross section enhancements.

II. NEUTRINO CROSS SECTIONS AND EFFECTIVE SOLID ANGLE

The dependence of neutrino induced events on the neutrino cross section has been the subject of much discussion, e.g., in Refs. [31–33]. One feature is that the probability of interaction is proportional to the neutrino nucleon cross section, however, the neutrino flux attenuation is also affected by the cross section.

Experimentally, the neutrino nucleon cross section has

been directly measured for $E_\nu < 450$ GeV [34]. A related measurement, the charged current interaction cross section for electrons in ep scattering at HERA translates to a neutrino cross section with $E_\nu = 27$ TeV incident on a proton at rest [35]. The moment transfer relevant to UHE neutrino scattering is characterized by the W-boson mass M_W . At $Q^2 \sim M_W^2$, the structure functions have been measured in the Bjorken x regime of x larger than a few times 10^{-3} . At the Large Hadron Collider, one expects measurements of the structure functions for $x > 10^{-5}$ for similar values of Q^2 . The reach in x at the Large Hadron Collider (LHC) extends to an equivalent neutrino energy $E_\nu \sim 10^8$ GeV, using the approximate correspondence that $2M_N E_\nu \sim M_W^2 \simeq \langle Q^2 \rangle$ [10]. We consider here neutrino energies $E_\nu \geq 10^8$ GeV, above kinematic regions probed even by the LHC experiments.

The neutrino cross section in the standard model, with a power law extrapolation of the structure functions at low x , has an approximate power law energy dependence [10, 11] $\sigma_{\nu N}^{\text{tot}} \simeq 1.57 \times 10^{-35} \text{ cm}^2 (E_\nu/\text{GeV})^{0.33}$. The neutrino interaction length is defined to be

$$L_\nu \equiv \frac{1}{\sigma_{\nu N}^{\text{tot}} N_A} . \quad (1)$$

This has the dimensions of g/cm^2 , or equivalently centimeters of water equivalent distance (cmwe), which can be converted to a distance by dividing by density. Rather than use a power law form, we use the charged current cross sections of Ref. [12], with the addition of the top quark contribution (on the order of a 30% correction at the highest energy [12, 13]). The charged current cross section, for high energies, is multiplied by an approximately energy independent constant of 1.43 to obtain the total neutrino-nucleon cross section [14]. The standard model neutrino interaction length is shown in Fig. 2. For an incident neutrino energy of 10^3 GeV, the tau neutrino cross section is only $\sim 5\%$ less than the muon neutrino cross sections [36]. We will be considering higher energies where we can use the same cross sections for all three neutrino flavors.

The importance of neutrino attenuation in the Moon or Earth can be seen with a comparison of the interaction length L_ν as a function of neutrino energy for the standard model cross section with the Earth and Moon diameters. The Earth diameter equals the neutrino interaction length for E_ν larger than a few tens of TeV. The Moon's diameter (in cmwe) equals the neutrino interaction length for an incident neutrino energy of a few times 10^6 GeV. Our focus will be on cosmogenic neutrinos at energies much higher than 10^6 GeV, so attenuation effects will be important in the evaluation of interaction rates, as we discuss in detail below. We note that the Earth's horizontal atmospheric depth is small on the scale of the neutrino interaction length, even at $E_\nu = 10^{12}$ GeV.

The cross section dependence of event rates is specific

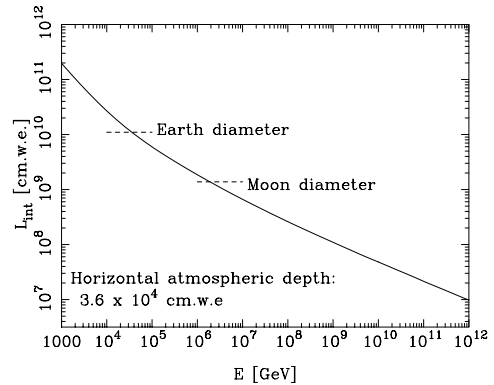


FIG. 2: The neutrino interaction length (in centimeters water equivalent distance) as a function of energy, with indications of the diameter of the Earth and Moon using the cross sections from Ref. [12].

to the signal and the possibility of neutrino regeneration through neutrino neutral current interactions and for tau neutrinos, through neutrino production and decay [31, 32, 37]. The neutral current neutrino regeneration can be approximately included via an effective cross section

$$\sigma \equiv \sigma_{\nu N}^{\text{eff}} = \kappa \sigma_{\nu N}^{\text{tot}}, \quad (2)$$

where we have taken σ to scale with energy as $\sigma_{\nu N}^{\text{tot}}$. In principle, κ depends on neutrino energy, but in practice at high energy, the differential cross section for neutrino neutral current interactions has an approximate scaling with neutrino energy the same way as the total cross section. We neglect the $\nu_\tau \rightarrow \tau \rightarrow \nu_\tau$ regeneration, which is typically not very important for steeply falling fluxes [37].

We can estimate κ in the standard model with some approximations. This is also outlined in the Appendix of Ref. [27]. The neutrino flux as a function of column depth X is

$$\begin{aligned} \frac{d\Phi_\nu(E, X(\theta))}{dX} &= -\frac{\Phi_\nu(E, X(\theta))}{L_\nu} \\ &+ \int_{E_\nu}^{\infty} dE' \Phi_\nu(E', X(\theta)) \frac{d\sigma_{NC}(E', E)}{dE} \end{aligned} \quad (3)$$

In the standard model, the neutral current cross section is approximately $r_{NC} = 0.3$ of the total cross section. Using

$$\frac{d\sigma_{NC}(E', E)}{dE} \simeq r_{NC} \sigma_{\nu N}^{\text{tot}}(E') \delta(E - (1 - \langle y \rangle) E') \quad (4)$$

where $y = (E' - E)/E'$ is the neutrino inelasticity, relating the change in neutrino energy when it interacts, normalized to the initial neutrino energy. At high energies,

$\langle y \rangle \simeq 0.2$. For a power law spectrum $\Phi_\nu(E, X(\theta)) \sim E^{-\gamma}$ and for a neutrino cross section which scales with energy as $\sigma_{\nu N}^{\text{tot}} \sim E^\delta$, Eq. (4) can be written as

$$\begin{aligned} \frac{d\Phi_\nu(E, X(\theta))}{dX} &= -\left(1 - r_{NC}(1 - \langle y \rangle)^{\gamma-1-\delta}\right) \frac{\Phi_\nu(E, X(\theta))}{L_\nu} \\ &= -\kappa \frac{\Phi_\nu(E, X(\theta))}{L_\nu}. \end{aligned} \quad (5)$$

When $\delta = 0.3$, as is approximately the case for the standard model, with $r_{NC} = 0.3$, $\kappa \simeq 0.74$ for a spectral index $\gamma = 2$. The value of κ is not very sensitive to the spectral index. It increases to $\kappa \simeq 0.84$ when $\gamma = 4$. We use $\kappa = 0.84$ in our evaluation below, and we define the attenuation distance λ to include the regeneration effect by

$$\lambda \equiv 1/\sigma N_A = L_\nu/\kappa. \quad (6)$$

We review here the scaling of upward event rates including attenuation as a function of the cross section. Schematically, event rates Γ for a detector of cross sectional area \mathcal{A} are given by

$$\begin{aligned} \Gamma &= \int dE_\nu d\Omega_\nu d\hat{A} \cdot \hat{n}(\theta_\nu) dr \mathcal{P}(E_\nu, \theta_\nu, r) \\ &\times \Phi_\nu(E_\nu, X(\theta_\nu)) \end{aligned} \quad (7)$$

where $\Phi_\nu(E_\nu, X)$ is the neutrino flux in units of neutrinos/(cm²s sr GeV), and $dr \mathcal{P}(E_\nu, \theta_\nu)$ is the probability the neutrino of energy E_ν produces a signal in the interval dr . The angle θ_ν is the incident angle of the neutrino flux with respect to vector normal to the cross sectional area of the detector. The probability to produce a signal depends linearly on the neutrino cross section for the specific signal (σ_s), so considering short distances $L = \int dr$, we can write $dr \mathcal{P}(E_\nu, \theta_\nu) = dr \sigma_s N_A \rho$. The effective volume of the detector is V , where $dV = dr d\mathcal{A}$. We consider detection near the surface, where for upward neutrino fluxes, the depth of the detector is negligible.

We start with a configuration of a detector near the surface which is approximately isotropic: where $\hat{A} \cdot \hat{n}$ is independent of the neutrino direction and where the pathlength of the neutrino in the detector of size $V = L^3$ is approximately independent of incident neutrino direction:

$$\mathcal{P}^{\text{iso}}(E_\nu, \theta_\nu, L) \simeq \mathcal{P}^{\text{iso}}(E_\nu, 0, L).$$

The neutrino flux accounting for attenuation, for an upward neutrino traversing a sphere and emerging with an angle θ_ν with respect to the normal to the surface is approximately

$$\Phi_\nu(E_\nu, X(\theta_\nu)) \simeq e^{-2R \cos \theta_\nu / \lambda} \Phi_\nu(E_\nu, 0) \quad (8)$$

for a flux incident on the Earth or Moon with column depth of the diameter of $2R$. For the Moon, $2R = d_M \rho_M$ for the diameter of the Moon $d_M = 3,480$ km and average

lunar density $\rho_M = 3.34$ g/cm³. Here, θ_ν is the zenith angle of the incident neutrino flux. We assume that the neutrino flux is isotropically incident on a spherical body (the Earth or Moon).

By factorizing the depth dependent neutrino flux as in Eq. (8), the integrand for an isotropic incident flux has a factor which includes the effective solid angle Ω_{eff} where

$$\begin{aligned} \frac{\Omega_{\text{eff}}^{\text{iso}}}{2\pi} &= \int_0^{\pi/2} d\theta_\nu \sin \theta_\nu e^{-2R \cos \theta_\nu / \lambda} \\ &= \frac{\lambda}{2R} \left(1 - \exp(-2R/\lambda)\right). \end{aligned} \quad (9)$$

The angular integral for a fixed energy (fixed λ) depends only on $2R/\lambda$. This is shown in Fig. 3 where the dashed line shows the quantity $\lambda/2R$. The dashed line is the scaling behavior of the integral for small interaction lengths compared to the diameter of the Earth or Moon ($\lambda/2R < 1/2$).

For detectors which are not isotropic, similar result is found. Consider the a detector schematically shown in Fig. 4, where the area is $\mathcal{A} = A$ and the detector thickness is d , the quantity $\hat{A} \cdot \hat{n} = \mathcal{A} \cos \theta_\nu$ appears in the integral, but now $\int dr \mathcal{P}(E_\nu, \theta_\nu, r) = \sigma_s N_A \rho d / \cos \theta_\nu$, assuming no neutrino attenuation through the depth of the detector. The combined angular dependence makes the integrand the same as for an isotropic detector, so $\Omega_{\text{eff}}^{\text{iso}}$ is the same for any isotropic upward neutrino flux incident on an underground detector. Eq. (9) shows that roughly, for a given λ/R , the zenith angles which contribute range between $\theta = 90^\circ$ and $\theta = \cos^{-1}(\lambda/2R)$ when $2R \gg \lambda$.

Combined with the neutrino interaction probability and the effective area $\mathcal{A} = \mathcal{A}_0$, the cross section dependence of the effective solid angle, for small interaction lengths relative to the column depth $2R$ is

$$\int dr \Omega_{\text{eff}}^{\text{iso}} \mathcal{P}(E_\nu, 0, r) \mathcal{A} \sim \mathcal{A}_0 \frac{\sigma_s}{\sigma} \frac{d\rho}{2R} \quad (10)$$

for isotropic incident fluxes. This agrees with the discussion of, e.g., Ref. [31], where it is noted that for large neutrino cross sections, the effective solid angle is reduced in just the proportion to the increase in event rate in the detection region in their discussion of upward shower events.

The slab configuration of Fig. 4 is relevant to neutrino induced radio Cherenkov signals. As we discuss below, radio signals are produced in the a thin layer of the lunar regolith on the surface facing the Earth. The depth of layer is characterized by the attenuation length of the radio signal, L_γ . Additional factors are required to account for the radio signal production and refraction at the surface, but schematically, the upward signal will be independent of the neutrino cross section at high energies, and it is proportional to L_γ .

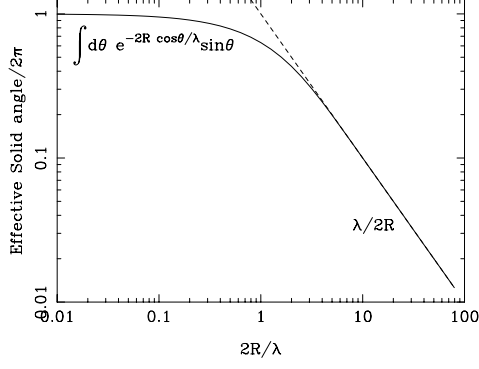


FIG. 3: The effective solid angle divided by 2π for an underground detector with an isotropic effective area, as a function of the ratio of the diameter (in water equivalent distance) to the attenuation distance (solid line). The dashed line shows $(\lambda/2R)$.

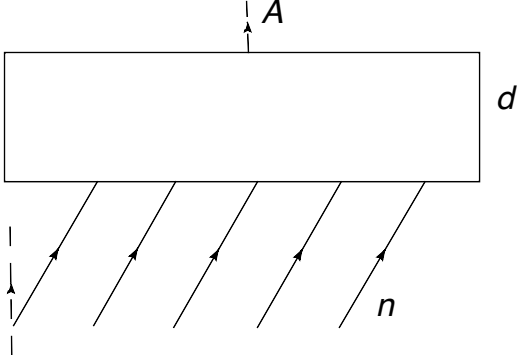


FIG. 4: A detector of area \mathcal{A} and depth d , with neutrinos incident in a directions characterized by \hat{n} which makes an angle θ_ν to the normal to the surface $\hat{\mathcal{A}}$.

III. LUNAR RADIO CHERENKOV SIGNALS FROM NEUTRINOS

To evaluate the neutrino event rate, we look at the effective aperture of the Moon evaluated by Gayley, Mutel and Jaeger in Ref. [27]. The effective aperture $A_M(E_\nu)$

combines the neutrino interaction probability, effective area (\mathcal{A}) and effective solid angle,

$$\Gamma = \int dE_\nu A_M(E_\nu) \Phi_\nu(E_\nu, X). \quad (11)$$

Eq. (11) also accounts for the radio Cherenkov signal production, attenuation and refractions at the lunar surface. $A_M(E)$ has units of $\text{sr}\cdot\text{km}^2$. GMJ[27] have shown that it is possible to parametrize the effective aperture for a lunar radio Cherenkov signal with the analytic form

$$\begin{aligned} A_M(E) &= A_0 \frac{(n_r^2 - 1)}{8n_r} \frac{L_\gamma}{L_\nu} f_0^3 \Delta_0 \\ &\times (\Psi_{ds} + \Psi_{dr} + \Psi_u) \\ &= A_{ds} + A_{dr} + A_u \\ &\equiv A_0 P(E). \end{aligned} \quad (12)$$

In this equation for the Moon, the index of refraction is $n_r = 1.73$ and the maximum lunar aperture is $A_0 = 4\pi(\pi R_M^2)$ for lunar radius $R_M = 1,740$ km. The photon interaction length (in g/cm^2 units) is $L_\gamma = 9 \text{ m} \times \rho/(\nu/\text{GHz})$ with a lunar regolith density of $\rho = 1.7 \text{ g}/\text{cm}^3$. We discuss our neutrino interaction length in detail below, but this factor of L_ν^{-1} carries the factor of σ_s in the probability for the neutrino to produce a signal. It is convenient to scale out a factor of A_0 and look at the energy dependent function $P(E)$.

The parameter f_0 is the ratio of the thickness of the Cherenkov cone at the electric field threshold ε_{\min} to the full thickness of the Cherenkov cone ($2\Delta_0$),

$$f_0 = \sqrt{\ln\left(\frac{0.6\varepsilon_0}{\varepsilon_{\min}}\right)} \quad (13)$$

where already the requirement that the electric field of the signal at the Earth is larger than the electric field threshold of the detector has been enforced. The quantity ε_0 depends on the distance to the moon $d = 3.84 \times 10^5$ km, the energy of the neutrino induced shower E_{shr} and the radio frequency of the radiation ν is

$$\begin{aligned} \varepsilon_0 &= 0.0845 \frac{\text{V}}{\text{m MHz}} \left[\frac{d}{\text{m}}\right]^{-1} \left[\frac{E_{shr}}{\text{EeV}}\right] \left[\frac{\nu}{\text{GHz}}\right] \\ &\times \left[1 + \left(\frac{\nu}{2.32 \text{ GHz}}\right)^{1.23}\right]^{-1} \end{aligned} \quad (14)$$

where $E_{shr} \simeq 0.2E_\nu$ is the approximate hadronic shower energy for neutrino interactions with nucleons in the lunar regolith. The quantity Δ_0 is the Cherenkov cone half width,

$$\Delta_0 = 0.05 \left[\frac{\text{GHz}}{\nu}\right] \left[1 + 0.075 \log_{10}\left(\frac{E_{shr}}{10^{10} \text{ GeV}}\right)\right]^{-1}. \quad (15)$$

The electric field threshold ε_{\min} of the detector depends on the collection area of the telescopes, the bandwidth and other features of the specific telescope or array of telescopes [27]. One example is Project RESUN [21] using the radio Expanded Very Large Array where $\varepsilon_{\min} \sim 10^{-8}$ V/m/MHz at 1.4 GHz.

There are three terms in eq. (12) representing the angular aperture fractions for downward neutrinos on a smooth surface (ds), downward neutrinos on a rough surface (dr) and upward neutrinos (u). They are respectively,

$$\begin{aligned}\Psi_{ds} &= f_0 \Delta_0 \\ \Psi_{dr} &= \frac{16}{3\pi^{3/2}} \sigma_0 = 0.96\sqrt{2} \tan^{-1}(0.14\nu^{0.22}) \\ \Psi_u &= \frac{16}{3} \frac{\lambda}{2R_M \rho_M} = \frac{16}{3} \frac{L_\nu}{2R_M \rho_M \kappa}.\end{aligned}\quad (16)$$

These terms were derived in the approximation that the neutrino interactions occur near the lunar surface, and that the spread of the Cherenkov cone is small, as is the incident neutrino direction relative to the horizontal to the lunar surface. This last approximation is valid as long as the neutrino interaction length is small compared to the lunar diameter.

Qualitatively, the prefactor accounts for the incident angles of the neutrinos, the cross sectional area of the moon, the interaction probability in the outer layer of the lunar regolith

$$P_{\text{eff}} \sim \frac{L_\gamma}{L_\nu} \sin \theta_c f_0^2,$$

the integral over the width of the Cherenkov cone giving $\sin \theta_c f_0 \Delta_0$ and the refraction effect on the solid angle subtended by the emerging radiation from inside the Moon (n_r). We recall that $\sin^2 \theta_c = (n_r^2 - 1)/n_r^2$.

For the upward effective aperture, the factor Ψ_u accounts for the reduced effective solid angle due to neutrino attenuation in the Moon. In fact,

$$\Psi_u = \frac{16}{3} \frac{\Omega_{\text{eff}}^{\text{iso}}}{2\pi}.\quad (17)$$

If the neutrino nucleon cross section is smaller than the standard model cross section, or at lower energies, the scaling of $\Omega_{\text{eff}}^{\text{iso}}$ with $(\lambda/2R)$ is modified, so we make the substitution of eq. (17) in the event rate to allow for lower cross sections (larger interaction lengths).

For neutrinos that are incident downward, some radio signal will emerge, namely the portion of the solid angle equal to the thickness of the Cherenkov cone. Without surface roughness, this is the only contributor to the radio signal, however, surface roughness permits the radio signal that would otherwise be lost to emerge. The approximate analytic result of Gayley et al. has the Ψ_{dr} contribution proportional to $\sigma_0 = \sqrt{2} \tan^{-1}(0.14\nu^{0.22})$, the surface roughness parameter in terms of the radio frequency ν in GHz. For $\nu = 1.5$ GHz, $\sigma_0 = 12.3^\circ = 0.21$

rad.

In Fig. 5, we show the effective aperture for (a) $\nu = 0.15$ GHz and (b) $\nu = 1.5$ GHz, for $\varepsilon_{\min} = 10^{-8}$ V/m/MHz. For the lower frequency, the downward neutrinos in the smooth approximation dominate, while for the higher frequency, roughness on the lunar surface transmits radio signals that would otherwise be lost. At the lower frequency end, the angular spread Cherenkov cone is broader than at higher frequencies, allowing more of downward signal to head towards Earth, even with an approximately smooth lunar surface. For the higher frequencies, the downward signals that emerge from the smooth surface approximation (ds) are smaller than the downward signals accounting for surface roughness. This comes from $f_0 \Delta_0 \sim 0.01 - 0.1$ which is small compared to the solid angle characterizing the surface roughness, $\sigma_0 \simeq 0.2$, as discussed by Gayley et al. [27]. In Fig. 6, for $\varepsilon_{\min} = 10^{-11}$ V/m/MHz, we show the effective aperture for the same two radio frequencies. The lower minimum detectable electric field allows a probe of a lower neutrino energy, where the flux of neutrinos is predicted to be much larger.

To show the dependence of the event rates on the neutrino nucleon cross section, we take as an example the radio frequency of $\nu = 1.5$ GHz and 100 hrs of viewing time. In Figs. 7 and 8, we use a cross section scaling factor of S of the standard model (SM) neutrino nucleon cross section,

$$\sigma_{\nu N} = S \sigma_{\nu N}^{SM},\quad (18)$$

to evaluate the rates for two choices of ε_{\min} , $\varepsilon_{\min} = 10^{-8}$ V/m/MHz and $\varepsilon_{\min} = 10^{-11}$ V/m/MHz. For the higher electric field threshold, we have shown results only for the highest cosmogenic neutrino flux in Fig. 1. For the lower threshold, we show results for both the upper and lower cosmogenic flux predictions.

Each of the separate contributions are shown: the dotted line show the “down smooth” contribution, the dot-dashed line shows the “down rough” contribution and the dashed line shows the “up” contribution. As discussed, the “up” contribution becomes independent of neutrino nucleon cross section when the cross section is large enough, while the “down” contributions scale linearly with the cross section. For low cross sections, attenuation of the upward neutrino flux is less prominent, so, for example, with $\varepsilon_{\min} = 10^{-11}$ V/m/MHz and $S \sim 0.01$, the upward event rate scales with the neutrino nucleon cross section.

The total numbers of events in one hundred hours are shown with the solid curves. The dots labeled CTW in each of the figures show a range of predictions using the uncertainty bands of Connolly, Thorne and Waters (CTW) discussed in Ref. [14]. The uncertainty is largest at the highest energies, probed with the lower electric field threshold. While the range of predictions spans a factor of about five, the overall predicted rate is quite low, even for the higher cosmogenic flux. The standard

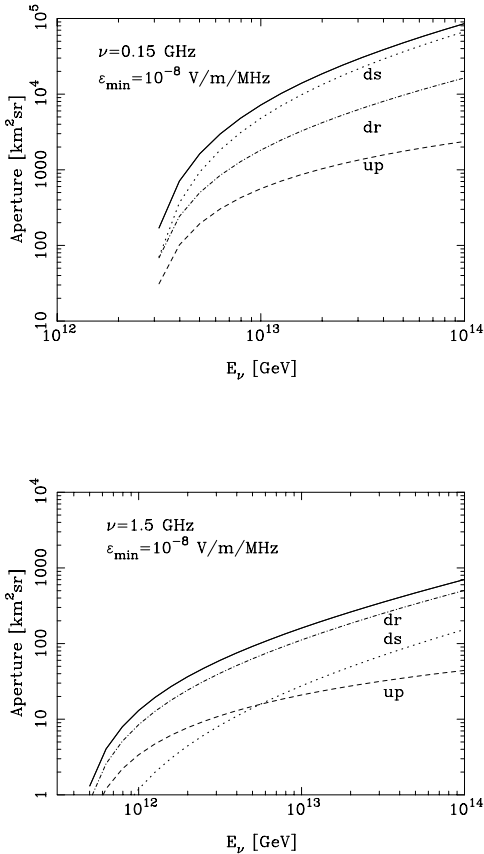


FIG. 5: The effective aperture as a function of neutrino energy for $\varepsilon_{\min} = 10^{-8}$ V/m/MHz and for two frequency choices: (a) $\nu = 0.15$ GHz and (b) $\nu = 1.5$ GHz. The solid line shows the total of the downward rough (dr, dot-dashed), downward smooth (ds, dotted) and upward neutrino (up, dashed) contributions.

model cross section (or the flux) must be enhanced by at least six orders of magnitude to get one predicted event in 100 hours. If it is the cross section that is enhanced to this degree, the neutrino interaction length becomes small compared to L_γ and the approximations used here for neutrinos do not apply. We discuss this possibility in the next section.

If an electric field detection threshold can be as low as $\varepsilon_{\min} = 10^{-11}$ V/m/MHz, then on the order of one event is predicted for $\nu = 1.5$ GHz. The standard model uncertainty is much less in the energy regime probed by this electric field sensitivity. Finally, we show the frequency dependence of eq. (11) using the standard model cross section for neutrinos and the high cosmogenic neutrino flux. In Fig. 9, we show the predicted number of events for 100 hours as a function of detected radio frequency. For standard model neutrino nucleon cross sections and the cosmogenic neutrino flux, the electric

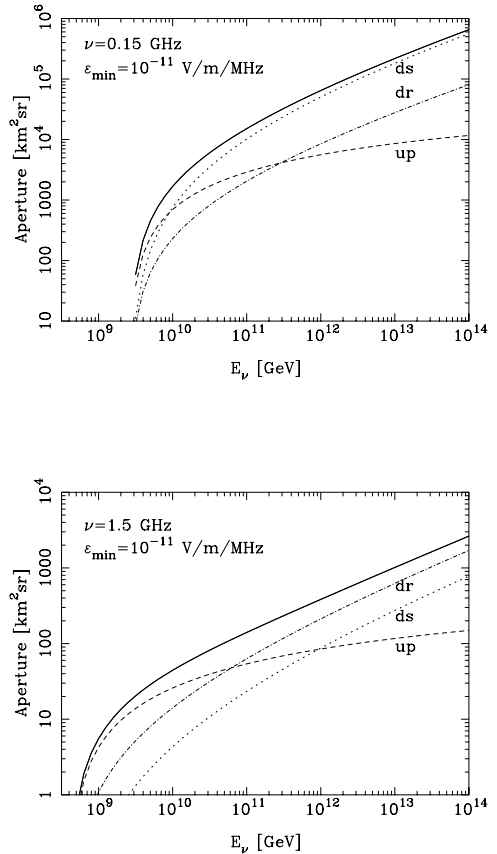


FIG. 6: The same as Fig. 5 but for $\varepsilon_{\min} = 10^{-11}$ V/m/MHz.

field detection threshold at Earth must be on the order of $\varepsilon_{\min} = 10^{-11} - 10^{-10}$ V/m/MHz for even one event in 100 hrs.

IV. LUNAR RADIO CHERENKOV SIGNALS FROM COSMIC RAY PROTONS

In the previous section, we saw that for a range of energies, depending on detection parameters, the downward neutrinos dominate the event rate. Contributions in the smooth case can dominate for some energies and for lower radio frequencies, while the surface roughness is important for the higher radio frequencies. Given that downward production of hadronic showers by neutrino interactions in the lunar regolith can produce observable radio Cherenkov signals at Earth, one should also consider the corresponding signals from hadronic showers induced by cosmic rays, the topic of this section. The Westerbork group has already used the absence of a cosmic ray induced radio Cherenkov signal to put a limit on the cosmic ray flux [29].

Our starting point is to treat the cosmic rays incident

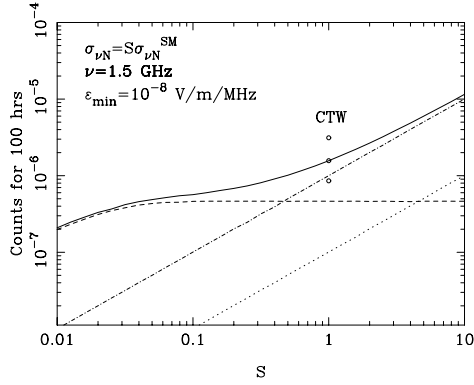


FIG. 7: The number of events for a 1.5 GHz signal with $\epsilon_{\min} = 10^{-8}$ V/m/MHz with the high cosmogenic flux from Fig. 1, with $E_\nu < 10^{14}$ GeV, as a function of $S = \sigma_{\nu N}/\sigma_{\nu N}^{SM}$. The up, down smooth and down rough contributions are as in Fig. 5 (b). The dots labeled CTW show the uncertainty bands of Ref. [14].

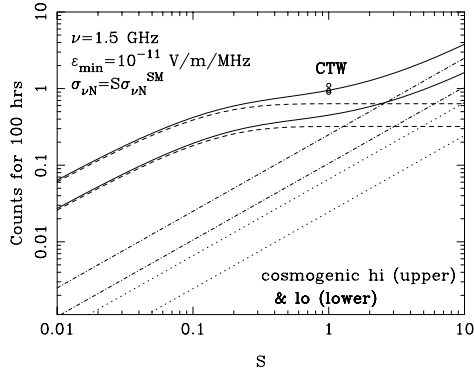


FIG. 8: The number of events for a 1.5 GHz signal as in Fig. 7, with $\epsilon_{\min} = 10^{-11}$ V/m/MHz with the low and high cosmogenic flux from Fig. 1, with $E_\nu < 10^{14}$ GeV, as a function of S .

on the lunar regolith with a flux shown in Fig. 1. The Pierre Auger Cosmic Ray Observatory analysis favors a composition of primarily iron nuclei at ultrahigh energies [38]. Iron nuclei incident with the same cosmic ray energy as a single proton will produce similar hadronic showers, so we use the cosmic ray flux of Ref. [30] assuming that the incident particles are protons carrying all the energy. For neutrino induced hadronic showers, we approximate the hadronic shower energy to be $E_{shr} \simeq 0.2E_\nu$. We will make the same approximation for cosmic rays, $E_{shr} \simeq 0.2E_{CR}$.

The essential difference between incident cosmic rays

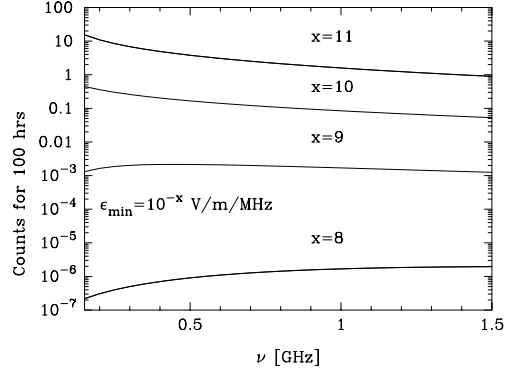


FIG. 9: The number of neutrino events as a function of radio frequency from cosmogenic neutrinos (high flux) with standard model interactions for $\epsilon_{\min} = 10^{-11} - 10^{-8}$ V/m/MHz.

and neutrinos is the difference between strong interaction and weak interaction cross sections. For $E_\nu = 10^{12}$ GeV, the neutrino interaction length in the standard model is on the order of 10^7 cmwe, as indicated in Fig. 2, however, for cosmic rays, the interaction length is $L_{CR} \simeq 50$ cmwe. This new scale makes some of the analytic approximations in Ref. [27] inapplicable to cosmic rays.

The short interaction length of cosmic rays makes attenuation of the flux important for downward cosmic rays, and it completely extinguishes the upward flux. We consider here the modifications to the effective aperture for the downward flux contribution, including attenuation in the regolith. Details of our evaluation appear in Appendix A.

Without attenuation, the target volume integral is governed by the maximum depth related to the photon attenuation length L_γ . In Ref. [27], the integral over the diameter of the moon r is replaced by an integral over the perpendicular distance to the surface h . In the small angle approximation, the maximum depth is approximately

$$h_{max} \simeq L_\gamma \sin \theta_c f_0^2 \left(1 - \frac{\Delta^2}{f_0^2 \Delta_0^2} \right), \quad (19)$$

where Δ is the polar angle from the Cherenkov peak. (See eq. (13) in Ref. [27].) This factor of L_γ arises because of the requirement that the radio Cherenkov signal emerge from the regolith. Without flux attenuation, the integral over h simply contributes a factor of h_{max} . These are some of the factors that appear in eq. (12) for neutrinos.

With flux attenuation, the integral over h in the evaluation of the effective aperture results in a factor of $|\sin \alpha| L_{CR}$, where α is the angle of the incident cosmic ray with respect to the horizontal, as in Ref. [27]. This modification of eq. (29) in Ref. [27], and subsequent

approximate integration, yields

$$P_{CR}(E) \simeq \frac{\sqrt{n_r^2 - 1}(f_0 \Delta_0)^3}{12} \left(1 + \frac{3}{4} \frac{\sigma_0^2}{f_0^2 \Delta_0^2} \right). \quad (20)$$

The first term in parenthesis is the smooth contribution, and the second term includes the additional contribution from surface roughness.

Eq. (20) shows that the probability for a cosmic ray to produce a signal is independent of the cosmic ray cross section, as long as cosmic ray flux attenuation is important on the scale of L_γ . This comes from two compensating factors. One factor of L_{CR} comes from the limit on the depth of targets from which there a signal, not because of radio wave attenuation, but because cosmic rays do not penetrate deeper in the regolith. The second factor is proportional to $\sigma_{CR} \sim 1/L_{CR}$ from the probability that the cosmic ray interacts to produce a radio Cherenkov signal.

In Fig. 10, we show the effective aperture for incident cosmic rays for $\nu = 0.15$ and 1.5 GHz and $\varepsilon_{\min} = 10^{-8}$ V/m/MHz, and in Fig. 11, we show the same for $\varepsilon_{\min} = 10^{-11}$ V/m/MHz. We see a similar dominance of the smooth contribution for the lower frequency, and rough contribution for the higher frequency, in the cosmic ray induced radio Cherenkov signals.

Based on these results for the effective aperture, we evaluate the number of events as a function of radio frequency induced by cosmic ray interactions. They are shown in Fig. 12 with the solid lines. For reference, the neutrino induced Cherenkov rates are shown with dashed lines. In all cases, the cosmic ray induced rates are larger than the neutrino induced rates. This is true at low and high radio frequencies, where either the smooth or rough downward contributions dominate. Our conclusion is that in the standard model of neutrino interactions with nucleons, the cosmic ray induced Cherenkov signals will overwhelm the cosmogenic neutrino induced signals, at least for the sample fluxes shown here. The lower electric field thresholds sample lower neutrino energies where there are larger fluxes of neutrinos, but there are even larger fluxes of cosmic rays at those energies. The higher energy thresholds suffer from low rates due to the low flux.

Theoretical predictions for neutrino induced event rates are enhanced if either the neutrino flux is much larger than shown, for example, in Fig. 1, or if the neutrino cross section is much larger than the standard model cross section. It is this second possibility that we explore in the next section.

V. RADIO CHERENKOV SIGNALS AND ENHANCED NEUTRINO CROSS SECTIONS

Enhanced neutrino-nucleon cross sections can arise in a variety of extensions of the standard model. Here, we consider the case of large extra dimensions. In theoretical

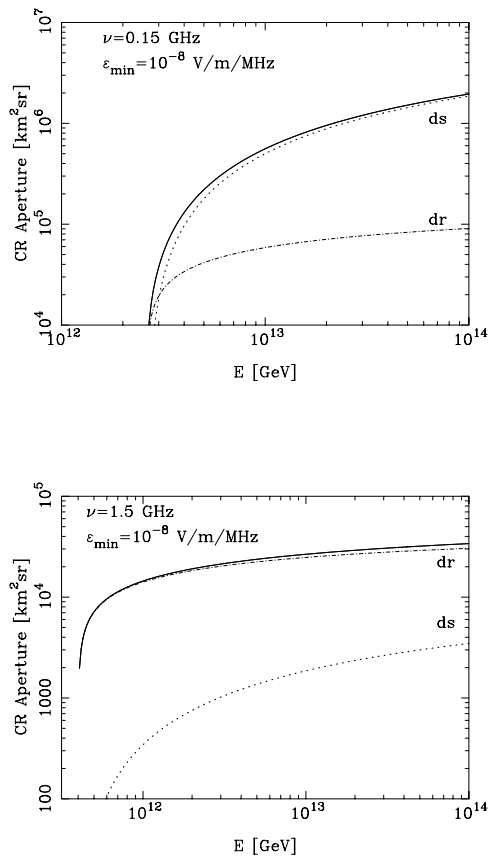


FIG. 10: The effective aperture as a function of cosmic ray energy for ($\varepsilon_{\min} = 10^{-8}$ V/m/MHz for (a) $\nu = 0.15$ GHz and (b) $\nu = 1.5$ GHz. The solid line shows the total of the downward rough (dr, dot-dashed) and downward smooth (ds, dotted). The cosmic ray effective aperture is independent of the cosmic ray cross section.

models with large extra dimensions and low scale gravity there is a possibility of creating a microscopic black hole in neutrino-nucleon interactions at very high energies [39]. In these models, gravitational interactions are modified and the four dimensional Planck scale (M_{Pl}) is related to the fundamental Planck scale in $4 + N_D$ dimension (M_D) by

$$M_{Pl}^2 = M_D^{N_D+2} V_{N_D}$$

where $V_{N_D} = (2\pi R)^{N_D}$ is the volume of the N_D -torus and R is the size of extra dimensions [39, 40]. When R is large (of the order of a millimeter), and the number of extra dimensions N_D is larger than 2, the fundamental Planck scale can be of the order of few TeV.

In high energy collisions, when particles with energies above M_D approach each other at the impact parameter which is less than the Schwarzschild radius in $4 + N_D$

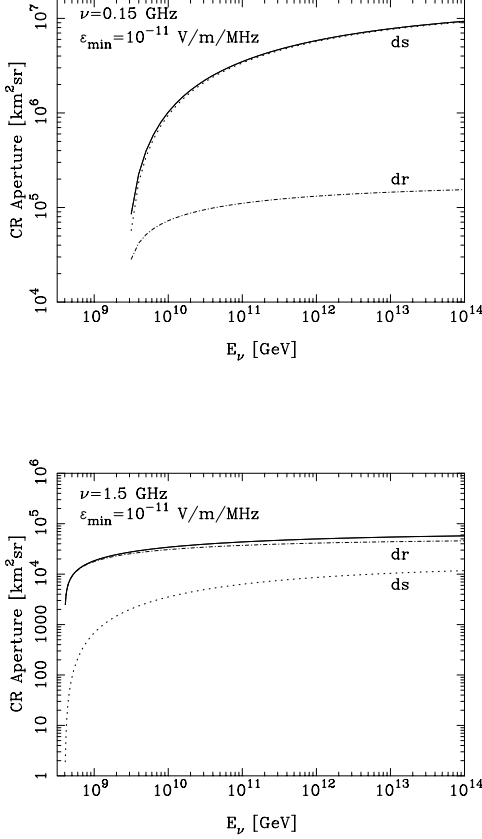


FIG. 11: The effective aperture as a function of neutrino energy for ($\varepsilon_{\min} = 10^{-11}$ V/m/MHz for (a) $\nu = 0.15$ GHz and (b) $\nu = 1.5$ GHz. The solid line shows the total of the downward rough (dr, dot-dashed) and downward smooth (ds, dotted).

dimensions, they can form the $4 + N_D$ dimensional black hole with mass M_{BH} [14, 41–45]. The radius r_S is given by [46]

$$r_S = \frac{1}{\sqrt{\pi}} \frac{1}{M_D} \left[\frac{M_{BH}}{M_D} \left(\frac{8\Gamma(\frac{N_D+3}{2})}{N_D+2} \right) \right]^{\frac{1}{N_D+1}}. \quad (21)$$

The neutrino-nucleon cross section for black hole production is given by [42]

$$\sigma(\nu N \rightarrow BH) = \sum_i \int_{\frac{(M_{BH}^{\min})^2}{s}}^1 dx \hat{\sigma}_i^{BH}(xs) f_i(x, Q^2), \quad (22)$$

where $\hat{\sigma}_i^{BH}$ is the neutrino-parton cross section given by [43]

$$\hat{\sigma}(\nu j \rightarrow BH) = \pi r_S^2 (M_{BH} = \sqrt{\hat{s}}) \theta(\sqrt{\hat{s}} - M_{BH}^{\min}), \quad (23)$$

s is the center of mass energy squared, $s = 2m_N E_\nu$, and $f_i(x, Q^2)$ is the parton distribution function for parton i . For semiclassical approximation to be valid, we need $M_{BH}^{\min} \gg M_D$.

Current limits on the M_D and N_D come from collider data [45, 47] as well as from the astrophysical observations. Strongest limits for $N_D < 4$ come from supernova cooling and neutron star heating, $M_D > 4$ TeV for $N_D = 4$, $M_D > 0.8$ TeV for $N_D = 5$ and for lower values of N_D , M_D is constrained to be much larger than few hundred TeV. Non-observation of the black hole production in cosmic neutrinos provide stringent limit for $N_D > 5$, $M_D > 1$ TeV [42].

We consider the parameter space (M_D, N_D) , for fixed M_{BH}^{\min} using the cross sections from Ref. [14] where $M_{BH}^{\min} = M_D$, to illustrate the consequences of enhanced neutrino nucleon cross sections given the highest cosmogenic neutrino flux shown in Fig. 1.

The neutrino-nucleon cross section for black hole production exceeds standard model cross section for neutrino energies above 10^6 GeV and is about two orders of magnitude larger than the standard model cross section at $E_\nu \sim 10^{11}$ GeV. In Fig. 13 we show the effect of the mini-black hole contribution to the neutrino-nucleon cross section on neutrino interaction length. The dashed line shows the interaction length for $N_D = 7$ and $M_D = 1$ TeV as calculated in Ref [14]. The dotted line shows the interaction length for the same (N_D, M_D) with the cross section taken from Ref. [41]. We note that the neutrino interaction length due to black hole production had strong energy dependence and at neutrino energies above 10^9 GeV, it is order of magnitude smaller than in the case of the standard model neutrino interactions. We use the neutrino cross sections due to black hole production from Ref. [14] as sample cross sections in what follows below.

The fact that the neutrino interaction length decreases to less than 10^4 cmwe above $E_\nu = 10^{12}$ GeV means that neither the cosmic ray approximation of strong attenuation nor the standard model neutrino evaluation of the effective downward aperture applies. The details of the evaluation of the effective aperture with the mini-black hole enhanced neutrino cross section contribution to the probability function $P_{BH\nu}(E)$ is shown in the Appendix.

To illustrate dependence of $P_{BH\nu}(E)$ on the neutrino interaction length, we evaluate $P_{BH\nu}(E)$ as a function of the ratio of the L_γ/L_ν . We show in Fig. 14 with the solid line the numerical evaluation of $P_{BH\nu}(E)$ from the formulas in GMJ with the modification of neutrino attenuation even over the distance scale of L_γ . The dashed horizontal lines show the what could be called the “cosmic ray limit,” when the non-standard model interactions make the neutrino interaction length small compared to L_γ . The dot-dashed lines show the “standard model neutrino limit” when $L_\nu \gg L_\gamma$ (the analytic expression of GMJ). In order from top to bottom, the curves show $(\varepsilon_{\min}, \nu)$ for $(10^{-11}, 0.15)$, $(10^{-8}, 0.15)$, $(10^{-11}, 1.5)$ and $(10^{-8}, 1.5)$ in units of (V/m/MHz, GHz). We note that the probability function for enhanced neutrino cross sections approaches

the cosmic ray approximation for $L_\gamma/L_\nu \geq 0.1$ (1.0) when $\varepsilon_{\min} = 10^{-8}$ V/m/MHz ($\varepsilon_{\min} = 10^{-11}$ V/m/MHz) and $\nu = 1.5$ GHz ($\nu = 0.15$ GHz). For lower values of L_γ/L_ν , the probability follows dependence on L_γ/L_ν similar to the the downward neutrino approximation of Eq. (12). As noted in Ref. [27], the approximate analytic solutions reproduced in our Eq. (12) are good to better than 25% compared to a numerical solution of the multidimensional integrals in their analytic expression. In evaluating neutrino induced Cherenkov signals with mini-black hole enhanced cross sections, we will use the numerical result (the solid line in Fig. 14) to ensure that we are properly accounting for the transition from weak to strong neutrino cross sections.

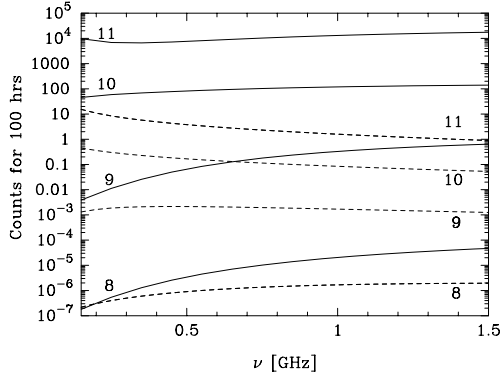


FIG. 12: The number of events as a function of radio frequency from the high flux of cosmogenic neutrinos (dashed) and from cosmic rays (solid), from top to bottom with $\varepsilon_{\min} = 10^{-11} - 10^{-8}$ V/m/MHz for standard model neutrino interactions.

In Fig. 15 we show number of cosmogenic neutrino events in 100 hrs for two frequency choices, $\nu = 0.15$ GHz (dashed) and $\nu = 1.5$ GHz (solid), as a function of the minimum electric field ε_{\min} . The parameters (N_D , M_D) are (1, 1 TeV), (7, 2 TeV) and (7, 1 TeV) from lowest to highest. The highest pair of solid and dashed lines for low ε_{\min} is for the cosmic ray induced events. We find that for $\nu = 1.5$ GHz (solid lines), the neutrino induced BH contributions are larger than the cosmic ray contributions for $\varepsilon_{\min} > 2 \times 10^{-9}$ V/m/MHz ($\varepsilon_{\min} > 6 \times 10^{-9}$ V/m/MHz) for $N_D = 7$ and $M_D = 1$ TeV ($M_D = 2$ TeV) black hole parameters. This comes from the highest energies considered, where the neutrino nucleon cross section is much bigger than the standard model, so the standard model neutrino interactions are negligible.

For $\nu = 0.15$ GHz, shown with the solid lines in Fig. 15, the neutrino induced BH contributions are larger than the cosmic ray induced Cherenkov signal for $\varepsilon_{\min} > 10^{-10}$ V/m/MHz, lower than the ε_{\min} for $\nu = 1.5$ GHz required for a signal from neutrinos with $N_D = 7$ and $M_D = 1$ TeV black hole parameters.

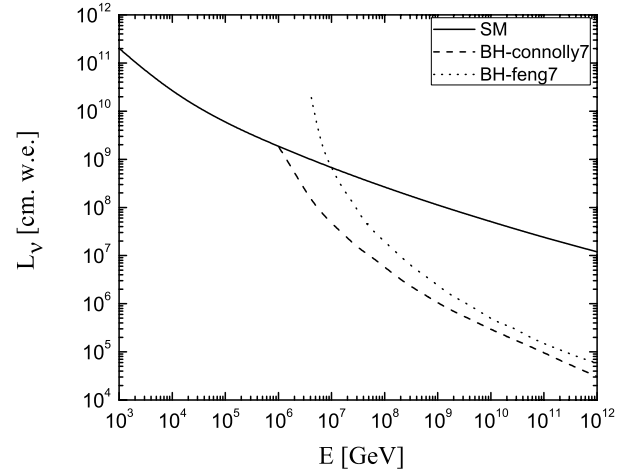


FIG. 13: The neutrino interaction length, with contributions from non-standard model mini-black hole production from Connolly, Thorne and Waters [14] and Feng [41] for $N_D = 7$, $M_D = 1$ TeV.

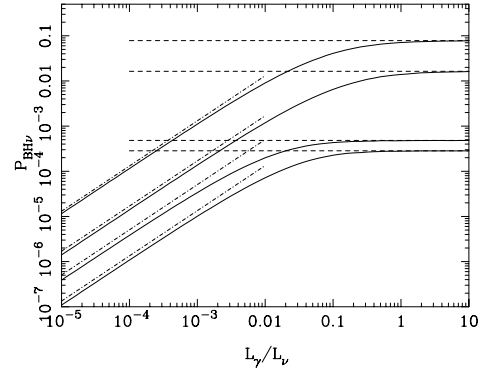


FIG. 14: The probability function which enters into the effective aperture, for neutrinos in which there is an enhancement of the neutrino cross section. The solid line shows the numerical evaluation, assuming $E = 10^{14}$ GeV, but varying the neutrino cross section relative to a fixed L_γ . The dashed horizontal line is the cosmic ray approximation of Eq. (20) and the dot-dashed line is the downward neutrino approximation of Eq. (12). In order from top to bottom, the curves show $(\varepsilon_{\min}, \nu)$ for $(10^{-11}, 0.15)$, $(10^{-8}, 0.15)$, $(10^{-11}, 1.5)$ and $(10^{-8}, 1.5)$ in units of (V/m/MHz, GHz).

From Fig. 15, we note that different BH parameters give similar dependence of the events on minimum electric field, with only difference being in the overall number of events. With 100 hrs, the BH enhanced neutrino signals dominate the cosmic ray background in the range of 40 events at the crossover for $\nu = 0.15$ GHz, while for $\nu = 1.5$ GHz, the crossover occurs at a fraction of an event level for the largest BH cross section considered

here.

In Fig. 16 we show the frequency dependence of the event rate for the lower and higher minimum electric field for three values of (N_D, M_D) . There is roughly an order of magnitude change in the neutrino induced event rates as a function of radio frequency for $\nu = 0.15 - 1.5$ GHz. Again we see in the figure that while event rates are higher for lower minimum electric fields, the cosmic ray background is much larger than the signal and thus dramatically lowering minimum electric fields does not favor the observation of cosmogenic neutrino induced Cherenkov signals.

Our conclusion is that for cosmogenic neutrino fluxes and neutrino cross sections enhanced by BH production with $N_D = 7$ and $M_D = 1$ TeV, the neutrino signal equals the cosmic ray background for $\varepsilon_{\min} \sim 10^{-10}$ V/m/MHz when $\nu = 0.15$ GHz, and the number of events is about 40. Thus, improvements in detector sensitivities would be required to observe the neutrino black hole enhanced signal. For a current detector capability of $\varepsilon_{\min} \sim 10^{-8}$ V/m/MHz, the enhanced neutrino cross section dominates the radio Cherenkov signal from the Moon relative to the cosmic ray background, however, the number of events in 100 hours is too small, of the order of 4×10^{-4} .

In addition to the cosmogenic neutrino flux that we have considered, there is a possibility that astrophysical sources produce larger neutrino fluxes via Fermi shock acceleration of the charged particles such as protons which collide with other protons or photons in a disk or a jet producing mesons which decay into neutrinos. Neutrino fluxes due to shock acceleration follow a power-law, i.e., $\Phi_\nu \sim E^{-2}$. We consider a neutrino flux which is currently below the Anita limit [18], i.e. ,

$$E^2 \Phi_\nu = 5 \times 10^{-7} \text{ GeV/cm}^2/\text{s/sr} . \quad (24)$$

In Fig. 17 we show the event rates for the neutrino flux in eq. (24) and for neutrino enhanced cross sections due to black hole production obtained with different black hole parameters (N_D, M_D) from Connolly et al. [14], as a function of the minimum electric field. We find that even for $\varepsilon_{\min} \sim 10^{-8}$ V/m/MHz, which is a current detector capability, for any frequency above 150 MHz the signal is above the cosmic background by several orders of magnitude. Total number of events varies between 1 (for $N_D = 1$ and $M_D = 1$ TeV) and 20 (for $N_D = 7$ and $M_D = 1$ TeV) for $\nu = 1.5$ GHz and between 40 and 200 for $\nu = 150$ MHz, depending on BH parameters. Lowering ε_{\min} results in only a slight increase in the event rates. For $\varepsilon_{\min} > 4 \times 10^{-10}$ the neutrino signal is above the cosmic ray background for any choice of BH parameters that we considered.

VI. DISCUSSION

We have used the formalism of GMJ in Ref. [27] to evaluate the effective aperture for lunar observations

from Earth of radio Cherenkov signals produced by neutrino interactions. The GMJ analytic effective aperture agrees qualitatively with the Monte Carlo results of James and Protheroe [48], as discussed in Ref. [27]. In the analytic approach, we have made a new evaluation of the lunar effective aperture for cosmic rays. This relies on the result of Ref. [29] that cosmic ray interactions in the lunar regolith produce radio Cherenkov signals that are indistinguishable from neutrino induced signals.

As Fig. 12 shows, the cosmic ray induced event rate always dominates the standard model neutrino event rate for the cosmogenic models of Ref. [9] for $\varepsilon = 10^{-8} - 10^{-11}$ V/m/MHz. Current capabilities for the electric field threshold are on the order of $\varepsilon_{\min} \sim 10^{-8}$ V/m/MHz. Decreasing ε_{\min} will not improve the capability of this lunar technique to detect the cosmogenic neutrino flux if the standard model interactions, e.g., with cross sections on the order of those reported in Refs. [10] and [12], are the only interactions responsible for the neutrino cross section. While lowering the minimum electric field increases the neutrino induced signal, it also increases the cosmic ray induced signal. The effective aperture for cosmic rays is independent of the cosmic ray cross section. Thus, the current discussion about the cosmic ray composition at the highest energies [38] will not impact our results as long as the cosmic rays interact strongly.

The radio Cherenkov technique can be exploited for lunar observations if the neutrino nucleon cross section is increased. We showed that for the choice of $M_D = 1$ TeV and $N_D = 7$ for BH production, an observable neutrino induced radio Cherenkov signal from the Moon is induced and it is larger than the cosmic ray induced background. For $\nu = 150$ MHz, this would require an instrumental improvement to reach $\varepsilon_{\min} \sim 10^{-10}$ V/m/MHz for the high cosmogenic flux of Fig. 1. We note that eventually enhancements of the neutrino cross section will push the rate evaluation into the “cosmic ray regime,” where the rate is independent of the cross section.

In Fig. 17, we showed that if both the neutrino cross section and the neutrino flux are enhanced, lunar radio Cherenkov techniques can make observations rather than set limits, even for $\varepsilon_{\min} \sim 10^{-8}$ V/m/MHz. Fig. 17 shows the observational capability as a function of ε_{\min} for two frequencies at the current limit on a neutrino flux of $E^2 \Phi_\nu = 5 \times 10^{-7}$ GeV/cm²/s/sr for a specific mini-blackhole model of neutrino cross section. In this model, the cross section enhancement relative to the standard model is $S = \sigma_{\nu N} / \sigma_{\nu N}^{SM} \sim 500$ for $E_\nu = 10^{12}$ GeV.

Taking a more generic approach, looking at the detectability as a function of S , we can see the capabilities of the lunar technique based on the GMJ formalism. In order to study the sensitivity of radio Cherenkov detection to the neutrino flux, we take neutrino flux of the form,

$$E^2 \Phi_\nu(E_\nu) = A \times 10^{-8} \text{ GeV/cm}^2/\text{s/sr} . \quad (25)$$

We investigate the value of A such that when $A = A_{100}$,

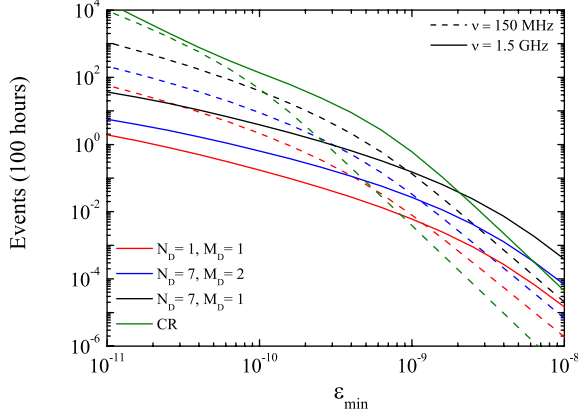


FIG. 15: Events in 100 hrs for $\nu = 150$ MHz (dashed) and 1.5 GHz (solid) as a function of ε_{\min} (in V/m/MHz) using enhanced neutrino cross sections from Connolly et al. [14], for three choices of black hole parameters, N_D and M_D . The high cosmogenic flux from Fig. 1 is used. The parameters (N_D, M_D) are (1, 1 TeV), (7, 2 TeV) and (7, 1 TeV) from lowest to highest event rates respectively. The top solid and dashed curve at $\varepsilon_{\min} = 10^{-11}$ V/m/MHz are the cosmic ray rates.

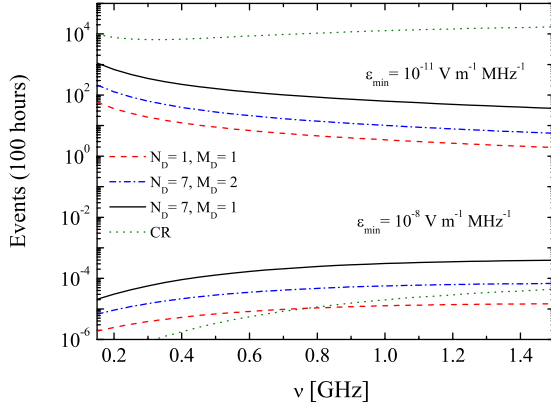


FIG. 16: Events in 100 hrs as a function of radio frequency for $\varepsilon_{\min} = 10^{-11}$ V/m/MHz (upper curves) and $\varepsilon_{\min} = 10^{-8}$ V/m/MHz (lower curves) for three choices of mini-blackhole parameters with the high cosmogenic neutrino flux. The cosmic ray induced event rate is shown with the dotted lines.

the theoretical prediction is one neutrino event for 100 hours of observation. We consider not only the total event rates but also the ratio of the cosmic ray induced signal over the neutrino induced signal,

$$R = \frac{\Gamma_{CR}}{\Gamma_{\nu}}. \quad (26)$$

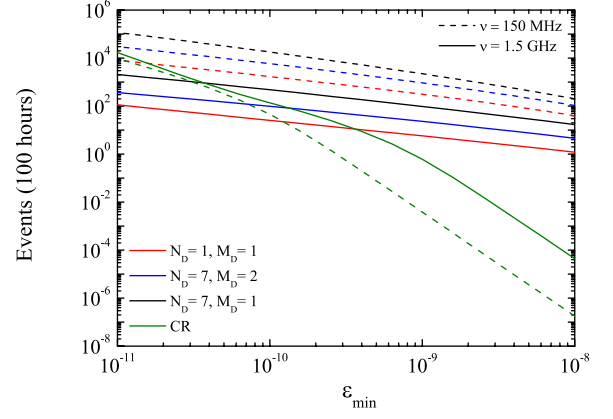


FIG. 17: Events in 100 hrs as a function of ε_{\min} for the enhanced neutrino cross section due to black hole production, for different values of (N_D, M_D) as in Fig. 15 and $E^2\Phi_{\nu} = 5 \times 10^{-7}$ GeV/cm²/s/sr. The lowest solid and dashed curves at $\varepsilon_{\min} = 10^{-8}$ V/m/MHz are the cosmic ray rates.

In Figs. 18 and 19, we show the two quantities, R and the minimum $A = A_{100}$ required for one neutrino event in 100 hrs, for the flux in eq. (25) for $\varepsilon_{\min} = 10^{-8}$ and 10^{-9} V/m/MHz, respectively, as a function of $S = \sigma_{\nu N}/\sigma_{\nu N}^{SM}$. The solid lines in these figures show the ratio R using the expression in eq. (A8) which produces the solid lines. This is labeled the “numerical” result. The dashed lines show the result using the “neutrino approximation” in which attenuation of the downward neutrino flux is not included. The dot-dashed lines show the value of A_{100} required to produce one event in 100 hours.

For $\varepsilon = 10^{-8}$ V/m/MHz, for both frequencies shown (1.5 GHz and 150 MHz), $R \ll 1$. The deviation between the solid and dashed lines shows the expected result that eventually, the neutrino rate does not increase with cross section because of attenuation of the downward flux in the Moon. The dot-dashed lines showing the minimum A for a neutrino flux with an analytic form following eq. (25) required for one neutrino event in 100 hrs also show the saturation effect due to attenuation. Even with large neutrino cross sections ($S \gg 1$), given 100 hrs, the minimum observable A for $\nu = 1.5$ GHz and $\varepsilon = 10^{-8}$ V/m/MHz is $A_{100} \simeq 1$. For values of S closer to 1, the minimum observable A is several hundred for 100 hrs of observation. This range of parameter space is already excluded by ANITA [17], however, not in this energy range. The lower frequency of $\nu = 150$ MHz probes a lower value of A , from $A = 1$ down to $A = 0.2$.

In Fig. 19 we show the same ratio R and A_{100} for $\varepsilon = 10^{-9}$ V/m/MHz. In this case the values of A_{100} needed to reach one neutrino event are much lower than in the case when $\varepsilon = 10^{-8}$ V/m/MHz. This is due to the fact that lowering ε we are probing neutrino fluxes at a lower energy where the flux is higher, as can be seen

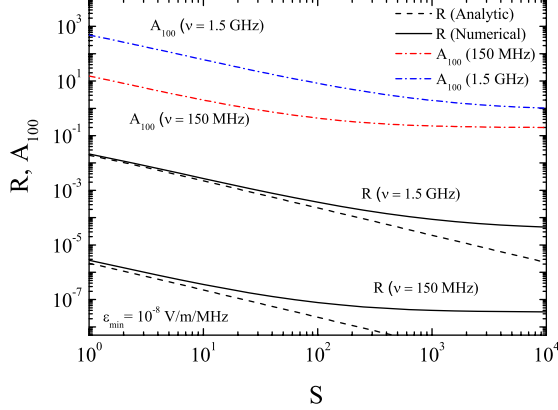


FIG. 18: For $E^2\Phi_\nu = A \times 10^{-8} \text{ GeV/cm}^2/\text{s/sr}$, the ratio $R = \Gamma_{CR}/\Gamma_\nu$ for $A = 1$ is shown with the solid lines where the full expression for the neutrino rate is used, while the dashed lines are evaluated using the “neutrino approximation,” with no attenuation for down-going neutrinos, as a function of $S = \sigma_{\nu N}/\sigma_{\nu N}^{SM}$ for $\varepsilon = 10^{-8} \text{ V/m/MHz}$. The dot-dashed lines show the minimum A to produce one neutrino event in 100 hrs, as a function of S .

from Fig. 1. However, for $\nu = 1.5 \text{ GHz}$, the ratio R is also much larger, and for $S < 10^2$, the CR background is larger than the neutrino signal. For lower frequencies, when $\nu = 150 \text{ MHz}$, for any value of S , including $S = 1$ which corresponds to the standard model neutrino cross section, the CR background is much smaller than the neutrino signal. In general, lower frequencies give larger event rates, and operating at lower frequency has this advantage in detecting neutrino fluxes. A theoretical advantage at the lower frequencies is that the event rate relies less on the surface roughness than for the higher frequencies. However, the observational challenge of atmospheric dispersion of the signal at $\nu = 150 \text{ MHz}$ is much more significant than at $\nu = 1.5 \text{ GHz}$.

There are several radio telescopes that have recently looked for very high energy neutrinos using the Moon as a target. The RESUN Project used the extended very large array (EVLA) with $\nu \sim 1.5 \text{ GHz}$ and $\varepsilon_{\min} = 10^{-8} \text{ V/m/MHz}$ [21]. The Westerbork Synthesis Radio Telescope (WSRT) operates in the frequency range of $115 - 180 \text{ MHz}$ and has reported limit on neutrino flux of $E^2\Phi_\nu \sim 10^{-6} \text{ GeV/cm}^2/\text{s/sr}$ [22]. The Lunaska experiment at the Australia Telescope Compact Array (ATCA) [24] is operating in the region $\nu = 1.2 - 1.8 \text{ GHz}$ and is expected to have sensitivities to lower neutrino fluxes than RESUN. At ultra-high energies ($E_\nu > 10^{14} \text{ GeV}$), NuMoon [23] which uses the Westerbork Synthesis radio Telescope in Netherlands, one of the most sensitive low-frequency experiment ($\nu = 113 - 175 \text{ MHz}$), will be able to place more stringent limit on the neutrino flux. LOFAR (Low Frequency Array), which covers frequencies between 120 MHz and 240 MHz and be-

tween 10 MHz and 80 MHz , is expected to lower their energy threshold down to 10^{11} GeV and with 30 days of data taking will be probing the neutrino flux down to $E^2\Phi_\nu \sim 3 \times 10^{-9} \text{ GeV/cm}^2/\text{s/sr}$ assuming standard model neutrino interactions [25]. Cosmic ray background for LOFAR is still sufficiently small relative to the neutrino signal. The advantage of LOFAR over RESUN, for example, is that it operates at low frequency and has longer observation time. However, it is important to note that lowering energy threshold down to 10^{10} GeV (i.e. lowering ε_{\min} below 10^{-10} V/m/MHz), would result in larger neutrino rates but the cosmic ray background would become significant. For neutrino fluxes lower than $E^2\Phi_\nu \sim 3 \times 10^{-9} \text{ GeV/cm}^2/\text{s/sr}$, LOFAR provides an excellent probe of physics beyond the Standard Model.

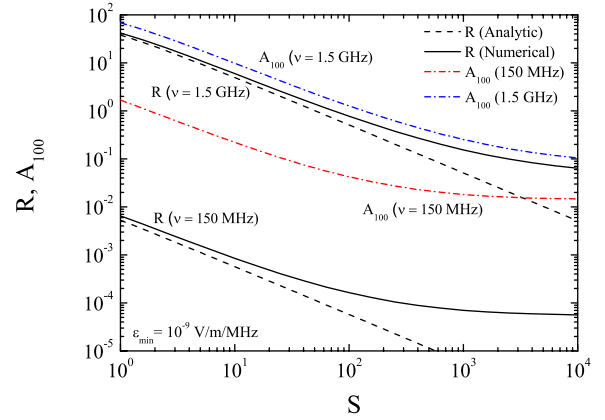


FIG. 19: The ratio R and the minimum A_{100} , as in Fig. 18 but for $\varepsilon = 10^{-9} \text{ V/m/MHz}$.

Acknowledgments

We would like to thank Ken Gayley, Robert Mutel and John Ralston. I.S. would like to thank Aspen Center for Physics for the hospitality. This work is supported in part by DOE contracts DE-FG02-91ER40664, DE-FG02-04ER41319 and DE-FG02-04ER41298.

Appendix A: Effective aperture for downward particle fluxes

Following Gayley, Jaeger and Mutel in Ref. [27], we evaluate the probability function $P(E)$ for downward incident particles with

$$P(E) = \frac{1}{\pi} \frac{L_\gamma}{L_\nu} \int_{-\infty}^0 d\alpha \cos \alpha \int_{-\infty}^{\infty} d\Delta \sin(\theta_c + \Delta) \times \int_0^{\infty} d\phi \int_0^{z_{max}} dz e^{-\tau_\nu} \mathcal{H}_R \mathcal{H}_D \xi, \quad (\text{A1})$$

(eq. (12) of Ref. [27]). For the sake of discussion, we will call the incident particles neutrinos. Here, α is the angle the incident neutrino makes with respect to the horizontal, with $\alpha < 0$ indicating “downward” neutrinos. The quantity Δ characterizes the polar angle of the interior ray solid angle relative to the cherenkov angle θ_c of the radio signal, and ϕ is its azimuthal angle. The factor ξ accounts for the fact that the radio signal encounters the lunar surface from the inside. The quantity z is the depth h in the lunar regolith, normalized by L_γ . In this equation, \mathcal{H}_R and \mathcal{H}_D are there to satisfy the conditions that the radio ray refracts (and does not totally internally reflect inside the moon), and that the rays are bright enough (detectable). Ref. [27] has \mathcal{H}_R written in terms of two more integrals, accounting for surface roughness so that the surface tilt polar angle is $\sigma = \sigma_0 w$ and the azimuthal tilt direction is ϕ' relative to a smooth surface, with

$$\mathcal{H}_R = \frac{2}{\pi^{3/2}} \int_0^{\pi/2} d\phi' \int_{-\infty}^{\infty} dw e^{-w^2} \mathcal{H}_{w,\phi'} . \quad (\text{A2})$$

The Heaviside step function $\mathcal{H}_{w,\phi'}$ enforces the requirement that the ray emerge from inside the Moon. Finally, the factor $e^{-\tau_\nu}$ accounts for the attenuation of the incident neutrino flux with

$$\tau_\nu = z \cdot L_\gamma / L_\nu \cdot 1/|\sin \alpha| . \quad (\text{A3})$$

The integral over z is straightforward, with

$$\int_0^{z_{max}} dz e^{-\tau_\nu} = \frac{|\sin \alpha| L_\nu}{L_\gamma} \left(1 - e^{-z_{max} L_\gamma / (|\sin \alpha| L_\nu)} \right) . \quad (\text{A4})$$

The quantity z_{max} is

$$z_{max} \simeq \sin \theta_c f_0^2 \left(1 - \frac{\Delta^2}{f_0^2 \Delta_0^2} \right) . \quad (\text{A5})$$

The result in eq. (A4) is the origin of the two limits, the “cosmic ray limit” and the “standard model neutrino

limit.” In the cosmic ray limit,

$$\int_0^{z_{max}} dz e^{-\tau_\nu} \simeq \frac{|\sin \alpha| L_\nu}{L_\gamma} \quad \text{CR limit} , \quad (\text{A6})$$

since the argument of the exponential is a large negative number with L_γ / L_ν large. The neutrino limit involves the expansion of the exponential in a power series, keeping the first non-zero term, so

$$\int_0^{z_{max}} dz e^{-\tau_\nu} \simeq z_{max} \quad \text{neutrino limit} . \quad (\text{A7})$$

For enhanced neutrino cross sections, where neither the cosmic ray nor neutrino limits are applicable, we numerically integrate eq. (A1) in the small angle limit, with the Heaviside functions enforced with downward incident angles to give

$$\begin{aligned} P(E) \simeq & \frac{n_r \sin \theta_c}{\pi^{3/2}} \int_0^{\pi/2} d\phi' \left[\int_{w_0}^{\infty} dw \int_{-f_0 \Delta_0}^{f_0 \Delta_0} d\Delta \right. \\ & \left. + \int_{-w_0}^{w_0} dw \int_{-w f_0 \Delta_0 / w_0}^{f_0 \Delta_0} d\Delta \right] \int_{\alpha_{min}}^0 d\alpha \\ & \times e^{-w^2} |\alpha| \left(1 - e^{-z_{max} L_\gamma / (|\alpha| L_\nu)} \right) \end{aligned} \quad (\text{A8})$$

where $\alpha_{min} = -\Delta - w \sigma_0 \cos \phi' = -\Delta - w/w_0$. Analytically, in the downward neutrino limit with $\sin \theta_0 = \sqrt{n_r^2 - 1}/n_r$, this yields

$$P(E) = P_\nu(E) \simeq \frac{n_r - 1}{8n_r} \frac{L_\gamma}{L_\nu} f_0^3 \Delta_0 (f_0 \Delta_0 + \frac{16}{3\pi^{3/2}} \sigma_0) .$$

In the cosmic ray limit, the integrals give

$$P(E) = P_{CR}(E) \simeq \frac{\sqrt{n_r^2 - 1} (f_0 \Delta_0)^3}{12} \left(1 + \frac{3}{4} \frac{\sigma_0^2}{f_0^2 \Delta_0^2} \right) .$$

-
- [1] See, e.g., B. Baret and V. Van Elewyck, Rept. Prog. Phys. **74**, 046902 (2011).
 - [2] K. Greisen, Phys. Rev. Lett. **16**, 748 (1966); G. T. Zatsepin and V. A. Kuzmin, JETP Lett. **4**, 78 (1966) [Pisma Zh. Eksp. Teor. Fiz. **4**, 114 (1966)].
 - [3] V. S. Beresinsky and G. T. Zatsepin, Phys. Lett. B **28**, 423 (1969); V. S. Berezinsky and G. T. Zatsepin, Yad. Fiz. **11**, 200 (1970).
 - [4] C. T. Hill and D. N. Schramm, Phys. Rev. D **31**, 564 (1985).
 - [5] R. J. Protheroe and P. A. Johnson, Astropart. Phys. **4**, 253 (1996).
 - [6] R. Engel, D. Seckel and T. Stanev, Phys. Rev. D **64**, 093010 (2001).
 - [7] D. Hooper, A. Taylor and S. Sarkar, Astropart. Phys. **23**, 11 (2005).
 - [8] A. V. Olinto, K. Kotera and D. Allard, arXiv:1102.5133 [astro-ph.HE], to appear in the Proceedings of NOW (Neutrino Oscillation Workshop) 2010, Nucl. Phys. B (Proc. Suppl.).
 - [9] K. Kotera, D. Allard and A. V. Olinto, JCAP **1010**, 013 (2010).
 - [10] R. Gandhi, C. Quigg, M. H. Reno and I. Sarcevic, Phys. Rev. D **58**, 093009 (1998); R. Gandhi, C. Quigg, M. H. Reno and I. Sarcevic, Astropart. Phys. **5**, 81 (1996).
 - [11] M. H. Reno, Nucl. Phys. Proc. Suppl. **143**, 407 (2005).
 - [12] Y. S. Jeong and M. H. Reno, Phys. Rev. D **81**, 114012 (2010).
 - [13] M. Gluck, P. Jimenez-Delgado and E. Reya, Phys. Rev. D **81**, 097501 (2010).
 - [14] A. Connolly, R. S. Thorne and D. Waters, Phys. Rev. D

- 83**, 113009 (2011).
- [15] P. Billoir [Pierre Auger Collaboration], J. Phys. Conf. Ser. **203**, 012125 (2010); J. Abraham *et al.* [Pierre Auger Collaboration], Phys. Rev. D **79**, 102001 (2009).
 - [16] R. Abbasi *et al.* [IceCube Collaboration], Phys. Rev. D **82**, 072003 (2010).
 - [17] P. W. Gorham *et al.* [ANITA collaboration], Phys. Rev. Lett. **103**, 051103 (2009).
 - [18] ANITA Collaboration (P.W. Gorham et al), Phys. Rev. D **82**, 022004 (2010).
 - [19] T. H. Hankins, R. D. Ekers and J. D. O’Sullivan, MNRAS **283**, 1027 (1996).
 - [20] P. W. Gorham, C. L. Hebert, K. M. Liewer, C. J. Naudet, D. Saltzberg and D. Williams, Phys. Rev. Lett. **93**, 041101 (2004).
 - [21] T. R. Jaeger, R. L. Mutel and K. G. Gayley, arXiv:0910.5949 [astro-ph.IM]; T. R. Jaeger, R. L. Mutel and K. G. Gayley, Astropart. Phys. **34**, 293 (2010).
 - [22] O. Scholten *et al.*, Phys. Rev. Lett. **103**, 191301 (2009).
 - [23] O. Scholten, *et al.*, Nucl. Instrum. Meth. **A604**, S102-S105 (2009).
 - [24] C. W. James *et al.*, Phys. Rev. D **81**, 042003 (2010).
 - [25] M. Mevius, *et al.*, “Detecting ultra high energy neutrinos with LOFAR,” Nucl. Instrum. Meth. in Physics Research **A** (in press); doi:10.1016/j.nima.2010.11.018.
 - [26] G. A. Askaryan, JETP **14**, 441 (1962); JETP **21**, 658 (1965).
 - [27] K. G. Gayley, R. L. Mutel and T. R. Jaeger, Astrophys. J. **706**, 1556 (2009).
 - [28] F. Halzen and S. R. Klein, Rev. Sci. Instrum. **81**, 081101 (2010) [arXiv:1007.1247 [astro-ph.HE]].
 - [29] S. ter Veen *et al.*, Phys. Rev. D **82**, 103014 (2010).
 - [30] J. Abraham *et al.* [The Pierre Auger Collaboration], Phys. Lett. B **685**, 239 (2010).
 - [31] S. Hussain, D. Marfatia, D. W. McKay and D. Seckel, Phys. Rev. Lett. **97**, 161101 (2006).
 - [32] A. Kusenko and T. J. Weiler, Phys. Rev. Lett. **88**, 161101 (2002).
 - [33] S. Palomares-Ruiz, A. Irimia and T. J. Weiler, Phys. Rev. D **73**, 083003 (2006).
 - [34] K. Nakamura *et al.* (Particle Data Group), J. Phys. G **37**, 075021 (2010).
 - [35] T. Ahmed *et al.* [H1 Collaboration], Phys. Lett. B **324**, 241 (1994); M. Derrick *et al.* [ZEUS Collaboration], Phys. Rev. Lett. **75**, 1006 (1995).
 - [36] Y. S. Jeong and M. H. Reno, Phys. Rev. D **82**, 033010 (2010).
 - [37] S. I. Dutta, M. H. Reno and I. Sarcevic, Phys. Rev. D **62**, 123001 (2000).
 - [38] J. Abraham *et al.* [The Pierre Auger Collaboration], arXiv:0906.2319, submission to the 31st International Cosmic Ray Conference, Lodz, Poland (July 2009)
 - [39] N. Arkani-Hamed, S. Dimopoulos and G. R. Dvali, Phys. Rev. D **59**, 086004 (1999).
 - [40] I. Antoniadis, N. Arkani-Hamed, S. Dimopoulos and G. R. Dvali, Phys. Lett. B **436**, 257 (1998); N. Arkani-Hamed, S. Dimopoulos and G. R. Dvali, Phys. Lett. B **429**, 263 (1998).
 - [41] L. A. Anchordoqui, J. L. Feng, H. Goldberg and A. D. Shapere, Phys. Rev. D **68**, 104025 (2003).
 - [42] See, e.g., J. L. Feng and A. D. Shapere, Phys. Rev. Lett. **88**, 021303 (2002); R. Emparan, M. Masip and R. Rattazzi, Phys. Rev. D **65**, 064023 (2002).
 - [43] See, e.g., J. Alvarez-Muniz, J. L. Feng, F. Halzen, T. Han and D. Hooper, Phys. Rev. D **65**, 124015 (2002); M. Kowalski, A. Ringwald and H. Tu, Phys. Lett. B **529**, 1 (2002); S. I. Dutta, M. H. Reno and I. Sarcevic, Phys. Rev. D **66**, 033002 (2002).
 - [44] S. Yoshida, Phys. Rev. D **82**, 103012 (2010).
 - [45] S. Dimopoulos and G. L. Landsberg, Phys. Rev. Lett. **87**, 161602 (2001); S. B. Giddings and S. D. Thomas, Phys. Rev. D **65**, 056010 (2002).
 - [46] R. C. Myers and M. J. Perry, Annals Phys. **172**, 304 (1986).
 - [47] V. Khachatryan *et al.* [CMS Collaboration], Phys. Lett. B **697**, 434 (2011).
 - [48] C. James and R. Protheroe, Astropart. Phys. **30**, 318 (2009).